Sensitivity analysis for trajectories of nonsmooth mechanical systems with simultaneous impacts

A hybrid systems perspective

Rijnen, Mark; Chen, Hao Liang; Van De Wouw, Nathan; Saccon, Alessandro; Nijmeijer, Henk

DOI
10.23919/acc.2019.8814388

Publication date
2019

Document Version
Final published version

Published in
Proceedings of the 2019 American Control Conference (ACC 2019)

2019 American Control Conference (ACC)
Philadelphia, PA, USA, July 10-12, 2019

Sensitivity analysis for trajectories of nonsmooth mechanical systems with simultaneous impacts: a hybrid systems perspective

Mark Rijnen, Hao Liang Chen, Nathan van de Wouw, Alessandro Saccon, Henk Nijmeijer

Abstract— **Sensitivity analysis for hybrid systems with state-triggered jumps is experiencing renewed attention for the control of robots with intermittent contacts. The basic assumption that enables this type of analysis is that jumps are triggered when the state reaches, transversally, a sufficiently smooth switching surface. In many scenarios of practical relevance, however, this switching surface is just piecewise smooth and, moreover, a perturbation of the initial conditions or the input leads to a different number of jumps than the nominal trajectory's. This work extends the sensitivity analysis in this context, under the assumptions that (i) at least locally, the intermediate perturbation-dependent jumps lead the system to reach always the nominal post-impact mode and (ii) once a switching and corresponding intermediate jump has occurred, its corresponding constraint remains active until reaching the nominal post-impact mode. Numerical simulations complement and validate the theoretical findings.**

I. Introduction

Hybrid systems [1] and, more specifically, hybrid systems with *state-triggered jumps* [2] can be used for controller design for robots with intermittent contacts performing juggling or dynamic walking motions [3], [4], [5], [6], [7].

Within this framework, the authors of this paper have recently proposed an analysis and control paradigm, named *reference spreading*, aiming at high performance control of mechanical systems experiencing impacts [8], [9], [10]. Reference spreading has the distinctive features of (i) being applicable to both periodic and nonperiodic trajectories with state-triggered events and of (ii) allowing for trajectories whose effective state dimension changes before and after each jump. For mechanical systems, this latter property means that one can deal with trajectories having phases of persistent contact.

At the core of reference spreading lies a sensitivity analysis for hybrid system trajectories with state-triggered jumps that can be used to infer local asymptotic stability [10]. The sensitivity analysis is performed under classical assumptions of transversality, no Zeno (i.e., no accumulation in time of jumps), and separate activation of the state-triggered switching functions [8], typically encountered also in hybrid optimal control and optimal motion planning for switching/jumping systems [11], [12], [13].

The key contribution of this paper is to relax the separate-switching assumption, showing that the sensitivity analysis can be performed even about a nominal trajectory whose events are triggered by the simultaneous activation of two or more switching functions. For mechanical systems, this simultaneous activation corresponds to physical impacts occurring at the same time in different points, such as when a humanoid robot dynamically lifts an object with both arms, or when a rigid object makes surface contact with another object at nonzero speed, with clear implications for the practical relevance of the developed theory. As the theory is not confined to mechanical systems, the results are presented here in a more general form.

Perturbing the initial conditions or control input destroys simultaneous switching. The number of jumps and modes traversed by a perturbed trajectory differs from that of the nominal trajectory. For a meaningful comparison of nominal and perturbed trajectories, we will introduce *multiscale hybrid time* (t, i, k), a specialization of hybrid time (t, j) [1].

Our analysis assumes that, at least locally, perturbed trajectories always return to the nominal post-impact mode after a perturbed sequence of jumps. Furthermore, once a constraint becomes active, it is assumed that it remains active until the nominal post-impact mode is reached. To ensure continuity with respect to the perturbations, we also assume that the reset maps satisfy a specific property, named *associativity*. We show that it is straightforward to find a nominal-trajectory and dynamical-system pair that satisfies these assumptions for mechanical systems with hard unilateral constraints experiencing simultaneous impacts.

To the best of the authors' knowledge, this is the first time a *sensitivity analysis* about a hybrid system's trajectory with simultaneous switching-function activation is proposed. In [14], a sensitivity analysis is proposed for non-differentiable switching functions and reset maps based on Nesterov's lexicographic differentiation, although there the sequence of modes is assumed to be fixed. In [15], [16], simultaneous switching-function activations are considered in the context of robotic applications and it is shown how, in the special case of imposing decoupling conditions on the system's inertia distribution and soft (i.e., spring-like) multi-contact points, perturbed trajectories are piecewise differentiable.

Mechanical systems with unilateral constraints can be described as measure differential inclusions (MDIs) [17], [18], [19], [20]. However, any attempt to recast our approach in this context is deemed for further investigation.

This paper is organized as follows. Section II presents the notion of multiscale hybrid time as well as new specific notation for the sensitivity analysis presented in Section III. Section IV presents a numerical example to illustrate and validate the concept.

M.W.L.M. Rijnen, H.L. Chen, N. van de Wouw, A. Saccon, and H. Nijmeijer are with the Department of Mechanical Engineering, Eindhoven University of Technology, The Netherlands. N. van de Wouw is also affiliated with the Department of Civil, Environmental, and Geo-Engineering, University of Minnesota, USA, and the Delft Center for Systems and Control, Delft University of Technology, The Netherlands

978-1-5386-7926-5/$31.00 ©2019 AACC

II. Background and Adopted Notation

We assume familiarity with hybrid systems and nonsmooth systems modeling [1], [18], [21]. Switching functions and reset maps determine when a jump has to occur and where to reinitialize the continuous state thereafter. This section introduces new terminology and notation (namely, *event character*, *mode descriptor*, *multiscale hybrid time*, and *historical notation*) that makes it possible to express the sensitivity analysis' results of Section III concisely, precisely, and more pleasantly for the eye. The reader is suggested to skim through this section at first read, returning to its specific content when necessary.

Nominal trajectory and event character. Consider a nominal state-input trajectory composed by absolutely continuous segments $(\boldsymbol{\alpha}(t,i),\boldsymbol{\mu}(t,i))$, $t\in[\tau_i,\tau_{i+1}]$, $i\in\{0,1,2,\dots\}$, defined over the time interval $[t_0,t_f]$, with $t_0=\tau_0$ and $t_f\leq+\infty$. We assume that the *nominal event times* τ_i are all distinct and do not accumulate in time (no Zeno). It is common to refer to t as the *regular time* and to i, a discrete counter, as the *discrete time* [1]. For a nominal trajectory with a finite number of events N, $\tau_{N+1}=t_f$.

Each τ_i, except for τ_0 and, if defined, also τ_{N+1}, corresponds to the simultaneous satisfaction of c_i switching conditions, expressed via c_i equalities of the form $\gamma_i^\eta=0$, with $\eta=2^{\nu-1}$, $\nu\in\{1,2,\dots,c_i\}$, where γ_i^η denotes a differentiable state-and-time-dependent *switching function*. As an example, when $c_i=3$, one writes $\gamma_i^{001}=0$, $\gamma_i^{010}=0$, and $\gamma_i^{100}=0$, where $2^{\nu-1}$ is written in the binary numeral system for reasons that will become clearer in the following paragraph. We will refer to c_i as the *character* of event i.

Hybrid dynamics and mode descriptor. Each segment of the nominal state-input trajectory $(\boldsymbol{\alpha},\boldsymbol{\mu})$ satisfies

$$\dot{\boldsymbol{x}}=\boldsymbol{f}(\boldsymbol{x},\boldsymbol{u},t),\qquad\qquad \boldsymbol{x}\in C,\tag{1}$$

where $\boldsymbol{x}$, $\boldsymbol{u}$, $\boldsymbol{f}$, and C are, respectively, short for $\boldsymbol{x}(t,i)\in\mathbb{R}^{n(s_i)}$, $\boldsymbol{u}(t,i)\in\mathbb{R}^{m(s_i)}$, ${}^{s_i}\boldsymbol{f}:\mathbb{R}^{n(s_i)}\times\mathbb{R}^{m(s_i)}\times\mathbb{R}\to\mathbb{R}^{n(s_i)}$, and $C=C(t):=\{\boldsymbol{x}\in\mathbb{R}^{n(s_i)}\mid\gamma_i^\eta(\boldsymbol{x}^\wedge,t)\geq0,\gamma_i^\zeta(\boldsymbol{x}^\wedge,t)\equiv0,\eta\in\eta(s_i),\zeta\notin\eta(s_i)\}$ with $n(s_i)$, $m(s_i)$, and $\eta(s_i)$ being the state dimension, input dimension, and the *set of inactive switching conditions* relative to the system mode whose *descriptor*, for the event i, is s_i. The mode descriptor $s_i\in\{0,1,2,\dots,2^{c_i}-1\}$ is a compact representation of the current mode of the system about the event i that includes only the set of switching conditions that can become active during the event i. The state dimension $n(s_i)$ is assumed to correspond to a representation of the system in mode s_i in minimal coordinates and consequently varies over time. We will write $s_i=s_i(t,i-1)$, when showing the explicit dependence on regular and discrete time is relevant. As done for the switching function index η, s_i will be expressed using binary numbers.

The index set of *inactive switching functions* associated to s_i, denoted $\eta(s_i)\subseteq\{2^0,2^1,\dots,2^{c_i-1}\}$, is obtained collecting the powers of two corresponding to the digits *zero* in the binary representation of s_i. As example, for $s_i=0110$, $\eta(s_i)=\{2^3,2^0\}$.

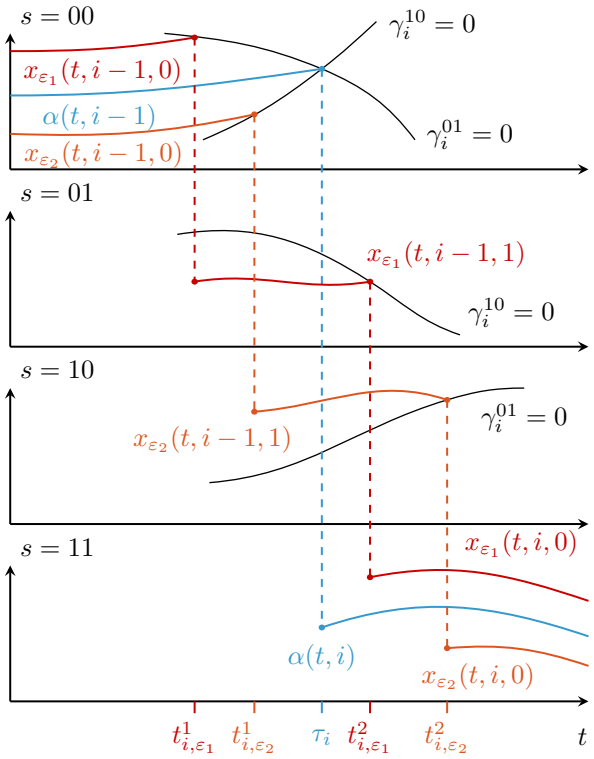

Fig. 1. Graphical representation of a nominal trajectory (blue) and two perturbed trajectories (red and orange) about a macro event with character two ($c_i=2$). See Section II for a detailed description of the symbols appearing in the figure. Note that $\gamma_i^{10}=0$ ($\gamma_i^{01}=0$) is drawn differently in $s=00$ and $s=01$ ($s=10$) on purpose, as the system evolves in different state-spaces for each of the four modes s.

The symbol $\equiv$ in the definition of the flow set C denotes the fact that not only the value of the switching function but also its time derivatives are identically zero, determining the size of the state space $\mathbb{R}^{n(s_i)}$ in which the constrained trajectories are allowed to evolve. To avoid redefining the switching functions γ_i^η for each possible constrained set, we make use of the notation $\boldsymbol{x}^\wedge\in\mathbb{R}^n$ to mean the lifted representation of the state $\boldsymbol{x}\in\mathbb{R}^{n(s_i)}$ in the unconstrained ambient space of dimension $n\geq n(s_i)$.

For the nominal trajectory $\boldsymbol{\alpha}$, the initial value of the descriptor for each event i is known in advance and we will write it as $\sigma_i=\sigma_i(t,i-1)=0\dots00$ (c_i digits zero). In (1), $s_i=\sigma_i$, $\eta(\sigma_i)=\{2^0,2^1,\dots,2^{c_i-1}\}$, and $(\boldsymbol{x},\boldsymbol{u})=(\boldsymbol{x}(t,i-1),\boldsymbol{u}(t,i-1))=(\boldsymbol{\alpha}(t,i-1),\boldsymbol{\mu}(t,i-1))$.

At event times, the continuous state is reset according to

$$\boldsymbol{x}^+=\boldsymbol{g}(\boldsymbol{x}^-,t),\qquad\qquad \boldsymbol{x}^-\in D,\tag{2}$$

where $\boldsymbol{x}^+$, $\boldsymbol{x}^-$, $\boldsymbol{g}$, and D are short for, respectively, $\boldsymbol{x}(t,i)\in\mathbb{R}^{n(s_i^+)}$, $\boldsymbol{x}(t,i-1)\in\mathbb{R}^{n(s_i^-)}$, ${}^{s_i^+\leftarrow s_i^-}\boldsymbol{g}:\mathbb{R}^{n(s_i^-)}\times\mathbb{R}\to\mathbb{R}^{n(s_i^+)}$, and $D=D(t):=\bigcup_{\beta\in\eta(s_i^-)}\{\boldsymbol{x}\in\mathbb{R}^{n(s_i^-)}\mid\gamma_i^\beta(\boldsymbol{x}^\wedge,t)=0,\gamma_i^\theta(\boldsymbol{x}^\wedge,t)\geq0,\gamma_i^\zeta(\boldsymbol{x}^\wedge,t)\equiv0,\theta\in\eta(s_i^-)\setminus\{\beta\},\zeta\notin\eta(s_i^-)\}$ where $s_i^+=s_i(t,i)$ and $s_i^-=s_i(t,i-1)$. The value of s_i^+ is determined by $\boldsymbol{x}^-$ and we assume that this map is deterministic and unique. Note that $s_i(t,i)$ differs from $s_{i+1}(t,i)$ although describing the same mode: for $\boldsymbol{\alpha}$, e.g., $s_i(t,i)=s_i^+=\sigma_i^+=1\dots11$ (c_i ones) while $s_{i+1}(t,i)=s_{i+1}^-=\sigma_{i+1}^-=0\dots00$ (c_{i+1} zeros).

Nearby trajectories and loss of simultaneity. Consider Fig. 1. The blue segments represent the nominal trajectory $\boldsymbol{\alpha}$ and the figure depicts a situation in which at time τ_i a character-two event occurs ($c_i = 2$), corresponding to the zeroing of two switching functions γ_i^{01} and γ_i^{10}.

The mode descriptor for the first segment of $\boldsymbol{\alpha}$ satisfies $s = 00$, while it satisfies $s = 11$ for the second segment. As mentioned previously, the digits 00 and 11 have to be interpreted as binary codes: 00 means that both switching functions are positive (inactive), while 11 means that both are zero (active). The length of the binary code associated to a mode descriptor allows immediately to deduce how many switching functions are relevant for a given event (i.e., its character) and also which switching conditions are active in that particular mode and which ones are not.

Fig. 1 also illustrates that the simultaneous satisfaction of switching conditions is easily lost by a perturbation in the state or input of the nominal trajectory. A nearby trajectory (e.g., $\boldsymbol{x}_{\varepsilon_1}$ in the figure) will likely encounter just a single switching function (γ^{01}), then jump to a new mode ($s = 01$), possibly encountering the other switching function (γ^{10}) and finally reaching the post-event mode of the nominal trajectory ($s = 11$). In the figure, a similar destiny is reserved for the perturbed trajectory $\boldsymbol{x}_{\varepsilon_2}$: in that case, the first switching function to become active is γ^{10}, the intermediate mode is $s = 10$, and only then also the switching function γ^{01} becomes active and the system reaches the nominal post-event mode $s = 11$. Note that at each mode transition, the state is reset according to a suitable reset map and the ante-event and post-event state dimensions are different. The situation clearly becomes more complicated with more switching conditions (it is actually *factorial* in the number of switching functions), but we will see in the next section that nevertheless it is possible to construct, straightforwardly, a relatively simple time-triggered system that is able to capture the local behavior of the hybrid system about $\boldsymbol{\alpha}$, generalizing the time-triggered linearization introduced in [8].

Multiscale hybrid time. How should different segments of a perturbed trajectory $\boldsymbol{x}_\varepsilon$ be numbered? It would be clearly still useful to use the counter i to distinguish, from a large-scale perspective, which event we are considering. However, as the number of intermediate events actually depends on the particular realization of the trajectory we are considering, it becomes necessary to introduce an additional counter to treat these intermediate transitions as of secondary importance. We introduce therefore a concept that we term *multiscale hybrid time*, through which each single segment of a state and input trajectory can be uniquely identified (the only work we are aware of employing a very similar concept is [19]). The multiscale hybrid time is denoted with (t, i, k). The *micro* counter k is initialized at zero and incremented by one every time a discrete event occurs, except when the system reaches the next expected nominal post-event mode. In the latter case, k is reset to zero and the *macro* counter i is incremented by one. Making use of the multiscale hybrid time, one can write $\boldsymbol{\alpha}(t, i)$ also as $\boldsymbol{\alpha}(t, i, 0)$. This extended notation will show its strength when willing to compare $\boldsymbol{\alpha}$ with a perturbed trajectory $\boldsymbol{x}_\varepsilon$, whose individual segments are denoted $\boldsymbol{x}_\varepsilon(t, i, k)$. An illustration of the use of the multiscale hybrid time is given in Fig. 1 for the two perturbed trajectories $\boldsymbol{x}_{\varepsilon_1}$ and $\boldsymbol{x}_{\varepsilon_2}$.

It is worth noting that the multiscale hybrid time (t, i, k) can be straightforwardly related to the classical notion of hybrid time (t, j) detailed in [1], via the simple relationship

$$j = j(i, k) = k + \sum_{\iota=0}^{i} l_\iota \tag{3}$$

with l_ι denoting the number of micro events (i.e., the maximum value of k plus one) during the macro event ι for the current trajectory at hand ($l_0 = 0$, by convention).

While the nominal macro-event times are denoted τ_i, the micro-event times for a given perturbed trajectory will be denoted t_i^1, t_i^2, ..., and $t_i^{l_i}$. If perturbed trajectories are parametrized by an index, such as ε in Fig. 1, then this parameter will appear as a subscript and we will write $t_{i,\varepsilon}^1$, $t_{i,\varepsilon}^2$, ..., $t_{i,\varepsilon}^{l_i}$. Note that, as in (3), l_i represents the total number of micro events about the i-th macro event for the trajectory under consideration. With a slight abuse of notation, we will write (t, i, l_i) to mean $(t, i + 1, 0)$: this allows to avoid specifying i when known from context, making use of just k with extended range 0 to l_i (in place of 0 to $l_i - 1$).

Using the multiscale hybrid time, each mode descriptor s_i is written $s_i(t, i - 1, k)$ or, for short, simply as s_i^k, pairing the notation t_i^k used for the micro event times. Note that we can then use $s_i^{l_i}$ to mean $s_i(t, i - 1, l_i) = s_i(t, i, 0)$.

Historical notation and growing sequences. Besides the notations s_i^k and t_i^k introduced above, it is useful to be able to indicate an entire mode sequence for the macro event i with a single symbol. To this end, we define S_i^k to mean $s_i^k \leftarrow s_i^{k-1} \leftarrow \cdots \leftarrow s_i^0$, where the initial descriptor $s_i^0 = 0 \ldots 00$ (as many 0's as the event character c_i) as all participating switching conditions are always inactive for $k = 0$. Accordingly, the historical notation ${}^{S_i^k}\boldsymbol{x}(t)$ will be used to refer to ${}^{s_i^k}\boldsymbol{x}(t) = \boldsymbol{x}(t, i - 1, k) \in \mathbb{R}^{n(s_i^k)}$ when it is also necessary to know that $\boldsymbol{x}(t, i - 1, k - 1) \in \mathbb{R}^{n(s_i^{k-1})}$, $\boldsymbol{x}(t, i - 1, k - 2) \in \mathbb{R}^{n(s_i^{k-2})}$, and so on, down to $\boldsymbol{x}(t, i - 1, 0) \in \mathbb{R}^{n(s_i^0)}$. When i is known from context, we simply write ${}^{S^k}\boldsymbol{x}(t)$. We can further specialize the historical notation to precisely indicate with one symbol a *specific* growing mode sequence starting from $s^0 = 0$. A mode sequence is called *growing* when, at each micro event, one (or more) switching condition becomes active, *while maintaining the status of all previously activated conditions unaltered*. We will use ${}^{\nu_k \nu_{k-1} \cdots \nu_1}S^k$ to denote the growing sequence whose elements are $s^\kappa = s^{\kappa-1} + \eta^\kappa$, $\eta^\kappa := 2^{\nu_\kappa - 1}$, $\kappa = \{1, 2, \ldots, k\}$. As example, for a character-3 event ($c_i = 3$), ${}^{132}S^3 = 111 \leftarrow 110 \leftarrow 010 \leftarrow 000$. We also allow, in case of simultaneous switching during a micro event, to indicate the participating switching function within brackets. As example, for a character-4 event sequence ($c_i = 4$), we write ${}^{3(41)2}S^3 = 1111 \leftarrow 1011 \leftarrow 0010 \leftarrow 0000$.

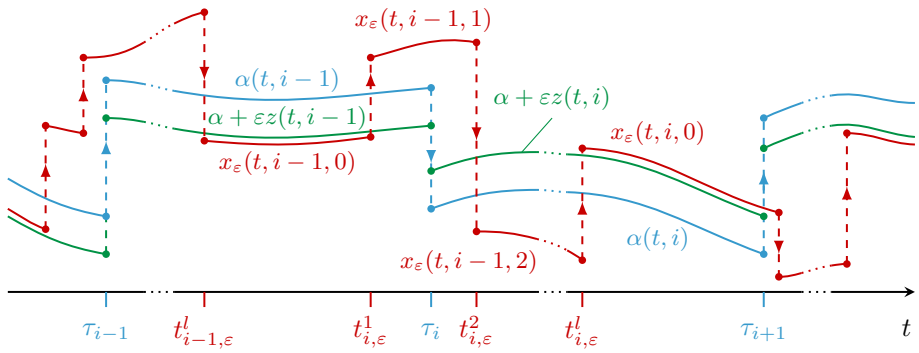

Fig. 2. Illustration of the first-order-approximation theorem. The perturbed trajectory $\boldsymbol{x}_\varepsilon$ (red) agrees with the sum (green) of the nominal trajectory $\boldsymbol{\alpha}$ (blue) and the positive homogenization $\boldsymbol{z}$, away from the time intervals where micro-events occur, up to first-order terms with respect to ε. Nominal macro-event times and perturbed micro-event times are indicated, respectively, as τ and t with corresponding subscripts as in the notation section.

III. The positive homogenization

In this section, we detail the sensitivity analysis about a trajectory with simultaneous switching-function activations. For sake of compactness, we will make extensive use of the notation introduced in Section II. The analysis is performed with respect to perturbations of the initial condition and control input. The central role in the analysis is played by a dynamical system with time-triggered state resets, named the *positive homogenization*. The positive homogenization extends the concept of time-triggered jumping linearization, introduced and employed in [8], [22], to hybrid systems with state-triggered jumps with character larger than one.

The sensitivity analysis is performed under the hypotheses that (i) the perturbed trajectories reach the nominal post-impact mode for sufficiently small perturbations and (ii) perturbed trajectories form growing mode sequences. For continuity of the state trajectory away from the jump times with respect to the perturbation, we require the jump map at each macro event to be *associative* as defined below.

***Definition** 1 (Jump map associativity):* Consider the jump map ${}^{p\leftarrow a}\boldsymbol{g}$ relating the ante-event state ${}^{a}\boldsymbol{x}$ with the post-event state ${}^{p}\boldsymbol{x}$ for a character-c macro event, namely

$$ {}^{p}\boldsymbol{x} = {}^{p\leftarrow a}\boldsymbol{g}({}^{a}\boldsymbol{x}, t). \tag{4}$$

In (4), the mode descriptors satisfy $a = 0\ldots00$ and $p = 1\ldots11$, with as many 0's and 1's as the event character c. The jump map ${}^{p\leftarrow a}\boldsymbol{g}$ is called *associative* about ${}^{a}\boldsymbol{x}$ at time t whenever, taking an arbitrary growing mode sequence $p = s^k \leftarrow s^{k-1} \leftarrow \cdots \leftarrow s^1 \leftarrow s^0 = a$, $k \leq c$, one has

$$ {}^{p}\boldsymbol{x} = \left({}^{p\leftarrow s^{k-1}}\boldsymbol{g}_t \circ \cdots \circ {}^{s^2\leftarrow s^1}\boldsymbol{g}_t \circ {}^{s^1\leftarrow a}\boldsymbol{g}_t \right)({}^{a}\boldsymbol{x}) \tag{5}$$

where $\boldsymbol{g}_t(\cdot) := \boldsymbol{g}(\cdot, t)$. ▲

Intuitively speaking, an associative jump map is one such that treating a simultaneous activation as a sequence of distinct activations leads to the same result. In Section IV, we will make use of the jump map corresponding to a simultaneous inelastic impact between a box and a plank that can be straightforwardly proven to be associative, suggesting that associative jump maps are not difficult to find in practice.

The concept of *nominal phantom segments* introduced next is required to detail the positive homogenization. For the reader interested in just grasping the essence of the sensitivity analysis, this definition can be skipped at first reading.

***Definition** 2 (Nominal phantom segments):* Given a trajectory $(\boldsymbol{\alpha}(t,i), \boldsymbol{\mu}(t,i))$ of (1)-(2), consider a macro event i and a growing mode sequence $S_i^k = s_i^k \leftarrow s_i^{k-1} \leftarrow \cdots \leftarrow s_i^0$. Let $\bar{\boldsymbol{\mu}}(t,i)$ denote a chosen *extended input* [10, Section III.A] for $\boldsymbol{\mu}(t,i)$, defined beyond the time interval $[\tau_i, \tau_i+1]$. The *pushing nominal phantom segment* of $(\boldsymbol{\alpha}, \boldsymbol{\mu})$ resulting from $\bar{\boldsymbol{\mu}}$ and S_i^k, denoted $({}^{S_i^k}_{\searrow}\bar{\boldsymbol{\alpha}}(t), {}^{S_i^k}_{\searrow}\bar{\boldsymbol{\mu}}(t))$, is the segment obtained via integration of the vector field ${}^{s_i^k}\boldsymbol{f}$ with input

$$ {}^{S_i^k}_{\searrow}\bar{\boldsymbol{\mu}}(t) := \begin{cases} \bar{\boldsymbol{\mu}}(t,i-1), & k \neq l_i \\ \bar{\boldsymbol{\mu}}(t,i), & k = l_i \end{cases} \tag{6}$$

and initial condition ${}^{s_i^k}\boldsymbol{\alpha}(\tau_i)$, the latter obtained as

$$ \begin{aligned} {}^{s_i^1}\boldsymbol{\alpha} &= {}^{s_i^1\leftarrow s_i^0}\boldsymbol{g}({}^{s_i^0}\boldsymbol{\alpha}, \tau_i) \\ &\vdots \\ {}^{s_i^k}\boldsymbol{\alpha} &= {}^{s_i^k\leftarrow s_i^{k-1}}\boldsymbol{g}({}^{s_i^{k-1}}\boldsymbol{\alpha}, \tau_i) \end{aligned} $$

where ${}^{s_i^0}\boldsymbol{\alpha}(\tau_i) = \boldsymbol{\alpha}(\tau_i, i-1, 0)$. In the expressions above, τ_i has been dropped as argument of ${}^{s_i^k}\boldsymbol{\alpha}$ for sake of brevity. Specularly, the *withdrawing*[1] *nominal phantom segment* $({}^{S_i^k}_{\nearrow}\bar{\boldsymbol{\alpha}}(t), {}^{S_i^k}_{\nearrow}\bar{\boldsymbol{\mu}}(t))$ is obtained integrating ${}^{s_i^k}\boldsymbol{f}$ from the initial condition ${}^{s_i^k}\boldsymbol{\alpha}(\tau_i)$ with input

$$ {}^{S_i^k}_{\nearrow}\bar{\boldsymbol{\mu}}(t) := \begin{cases} \bar{\boldsymbol{\mu}}(t,i-1), & k = 0 \\ \bar{\boldsymbol{\mu}}(t,i), & k \neq 0 \end{cases}. \tag{7}$$

***Remark** 1:* It is straightforward to verify that, whenever ${}^{s_i^l\leftarrow s_i^0}g(\cdot,\tau)$ is associative, ${}^{S_i^k}_{\searrow}\boldsymbol{\alpha}(\tau) = {}^{S_i^k}_{\nearrow}\boldsymbol{\alpha}(\tau)$ for any sequence S_i^k, so that the subscripts $\searrow$ and $\nearrow$ can be dropped for $t = \tau$ with no ambiguity. △

***Definition** 3 (Push-and-withdraw sequence):* Given the nominal trajectory $(\boldsymbol{\alpha}(t,i), \boldsymbol{\mu}(t,i))$ satisfying (1) and (2), an associated *push-and-withdraw sequence* V is an ordered

[1]In words, a pushing input ${}_{\searrow}\bar{\mu}$ waits until the last micro event before switching to the next nominal post-impact input. A withdrawing input ${}_{\nearrow}\bar{\mu}$ switches immediately to the the next nominal post-impact input.

set that, for each macro event i, associates a pushing ($\searrow$) or withdrawing ($\nearrow$) symbol. ▲

A nominal trajectory such that each jump map is associative at each nominal jump time, in the sense of Definition 1, and that intersects transversally the level set zero of the switching functions [10] will be called an *associative transversal nominal trajectory*. For such a nominal trajectory, we can extend the sensitivity equations in [8] to form its associated positive homogenization as follows.

***Definition** 4 (Positive homogenization):* The positive homogenization of (1)-(2) about the associative transversal nominal trajectory $(\boldsymbol{\alpha}(t,i), \boldsymbol{\mu}(t,i))$ with push-and-withdraw sequence V is

$$
\begin{aligned}
{}^{a}\dot{\boldsymbol{z}} &= {}^{a}\boldsymbol{A}(t)\,{}^{a}\boldsymbol{z} + {}^{a}\boldsymbol{B}(t)\,{}^{a}\boldsymbol{v}, \qquad \tau_{-1} \le t \le \tau, && (8)\\
{}^{p}\boldsymbol{z} &= {}^{p\leftarrow a}\boldsymbol{h}({}^{a}\boldsymbol{z}, t), \qquad t = \tau, && (9)\\
{}^{p}\dot{\boldsymbol{z}} &= {}^{p}\boldsymbol{A}(t)\,{}^{p}\boldsymbol{z} + {}^{p}\boldsymbol{B}(t)\,{}^{p}\boldsymbol{v}, \qquad \tau \le t \le \tau_{+1}, && (10)
\end{aligned}
$$

where ${}^{p\leftarrow a}\boldsymbol{h}({}^{a}\boldsymbol{z}, \tau)$ is a positively homogeneous map in $\boldsymbol{z}$ (detailed below), $\tau_{-1} = \tau_{i-1}$, $\tau = \tau_i$, $\tau_{+1} = \tau_{i+1}$,

$$
\begin{aligned}
{}^{a}\boldsymbol{A}(t) &= D_1\,{}^{a}\boldsymbol{f}({}^{a}\boldsymbol{\alpha}(t), {}^{a}\boldsymbol{\mu}(t)),\\
{}^{a}\boldsymbol{B}(t) &= D_2\,{}^{a}\boldsymbol{f}({}^{a}\boldsymbol{\alpha}(t), {}^{a}\boldsymbol{\mu}(t)),\\
{}^{p}\boldsymbol{A}(t) &= D_1\,{}^{p}\boldsymbol{f}({}^{p}\boldsymbol{\alpha}(t), {}^{p}\boldsymbol{\mu}(t)),\\
{}^{p}\boldsymbol{B}(t) &= D_2\,{}^{p}\boldsymbol{f}({}^{p}\boldsymbol{\alpha}(t), {}^{p}\boldsymbol{\mu}(t)),
\end{aligned}
$$

with D_1 and D_2 denoting differentiation with respect to first and second arguments and where

$$
\begin{aligned}
{}^{a}\boldsymbol{\alpha}(t) &= \boldsymbol{\alpha}(t, i-1), \qquad & {}^{a}\boldsymbol{\mu}(t) &= \boldsymbol{\mu}(t, i-1),\\
{}^{p}\boldsymbol{\alpha}(t) &= \boldsymbol{\alpha}(t, i), & {}^{p}\boldsymbol{\mu}(t) &= \boldsymbol{\mu}(t, i),
\end{aligned}
$$

and ${}^{a}\boldsymbol{f}(\boldsymbol{x},\boldsymbol{u},t) = {}^{\sigma_i^-}\boldsymbol{f}(\boldsymbol{x},\boldsymbol{u},t)$, and ${}^{p}\boldsymbol{f}(\boldsymbol{x},\boldsymbol{u},t) = {}^{\sigma_i^+}\boldsymbol{f}(\boldsymbol{x},\boldsymbol{u},t)$ with $\sigma_i^- = 0\ldots00$ and $\sigma_i^+ = 1\ldots11$ (both zeros and ones repeated c_i times). Furthermore, in (8)-(10), ${}^{a}\boldsymbol{z}(t) = \boldsymbol{z}(t, i-1) \in \mathbb{R}^{n(s_{i-1})}$, ${}^{a}\boldsymbol{v}(t) = \boldsymbol{v}(t, i-1) \in \mathbb{R}^{m(s_{i-1})}$, ${}^{p}\boldsymbol{z}(t) = \boldsymbol{z}(t, i) \in \mathbb{R}^{n(s_i)}$, ${}^{p}\boldsymbol{v}(t) = \boldsymbol{v}(t, i) \in \mathbb{R}^{m(s_i)}$, the initial condition is $\boldsymbol{z}(\tau_0, 0) = \boldsymbol{z}_0 \in \mathbb{R}^{n(s_0)}$, $\tau_0 = t_0$, and, in case of a nominal trajectory $(\boldsymbol{\alpha}, \boldsymbol{\mu})$ with a finite number N of macro events, $\tau_N = t_f \le \infty$. The positively homogeneous map can always be written as ${}^{p\leftarrow a}\boldsymbol{h}({}^{a}\boldsymbol{z}, \tau) = {}^{p\leftarrow a}\boldsymbol{H}({}^{a}\boldsymbol{z}, \tau)\,{}^{a}\boldsymbol{z}$ with ${}^{p\leftarrow a}\boldsymbol{H}({}^{a}\boldsymbol{z}, \tau)$ a suitable state-dependent matrix gain. For a character-2 event (for which $p = 11$ and $a = 00$), we get

$$
{}^{11\leftarrow 00}\boldsymbol{H}(\boldsymbol{z},t) = \begin{cases} {}^{11\leftarrow 00}_{(21)\,S^1}\boldsymbol{G}, & {}^{1}S^1\boldsymbol{a}^T\boldsymbol{z} = {}^{2}S^1\boldsymbol{a}^T\boldsymbol{z} \\ {}^{11\leftarrow 01}_{21\,S^2}\boldsymbol{G}\,{}^{01\leftarrow 00}_{1\,S^1}\boldsymbol{G}, & {}^{1}S^1\boldsymbol{a}^T\boldsymbol{z} < {}^{2}S^1\boldsymbol{a}^T\boldsymbol{z} \\ {}^{11\leftarrow 10}_{12\,S^2}\boldsymbol{G}\,{}^{10\leftarrow 00}_{2\,S^1}\boldsymbol{G}, & {}^{2}S^1\boldsymbol{a}^T\boldsymbol{z} < {}^{1}S^1\boldsymbol{a}^T\boldsymbol{z} \end{cases}. \qquad (11)
$$

The single-jump gains ${}^{s^+\leftarrow s^-}_{S^k}\boldsymbol{G}$ and vectors ${}^{S^k}\boldsymbol{a}$ are detailed in the following exposition. Each single-jump gain ${}^{s^+\leftarrow s^-}_{S^k}\boldsymbol{G}$ in (11), with $S^k = s^k \leftarrow s^{k-1} \leftarrow \cdots \leftarrow s^0$ (see Section II) where $s^+ = s^k$ and $s^- = s^{k-1}$, equals

$$
{}^{s^+\leftarrow s^-}_{S^k}\boldsymbol{G} := D_1\boldsymbol{g}^- - \frac{\dot{\boldsymbol{g}}^- - \boldsymbol{f}^+}{\dot{\gamma}-} D_1\gamma^- \qquad (12)
$$

where, defining $R^{k-1} = s^{k-1} \leftarrow \cdots \leftarrow s^0$,

$$
\begin{aligned}
\boldsymbol{f}^+ &:= {}^{s^+}\boldsymbol{f}({}^{S}\boldsymbol{\alpha}(\tau), {}^{S}_{\rightarrow}\boldsymbol{\mu}(\tau), \tau), && (13)\\
\boldsymbol{f}^- &:= {}^{s^-}\boldsymbol{f}({}^{R}\boldsymbol{\alpha}(\tau), {}^{R}_{\rightarrow}\boldsymbol{\mu}(\tau), \tau), && (14)\\
\dot{\boldsymbol{g}}^- &:= D_1\boldsymbol{g}^- \cdot \boldsymbol{f}^- + D_2\boldsymbol{g}^- \cdot 1, && (15)\\
\dot{\gamma}^- &:= D_1\gamma^- \cdot \boldsymbol{f}^- + D_2\gamma^- \cdot 1, && (16)\\
D_\iota\boldsymbol{g}^- &:= D_\iota\,{}^{s^+\leftarrow s^-}\boldsymbol{g}({}^{R}\boldsymbol{\alpha}(\tau), \tau), \qquad \iota = \{1,2\}, && (17)\\
D_\iota\gamma^- &:= D_\iota\gamma^{\eta(s^+\leftarrow s^-)}({}^{R}\boldsymbol{\alpha}(\tau), \tau), \qquad \iota = \{1,2\}, && (18)
\end{aligned}
$$

with $({}^{S}\boldsymbol{\alpha}, {}^{S}_{\rightarrow}\boldsymbol{\mu})$ and $({}^{R}\boldsymbol{\alpha}, {}^{R}_{\rightarrow}\boldsymbol{\mu})$ denoting nominal phantom segments with $\rightarrow$ to be interpreted as $\searrow$ or $\nearrow$ depending on the push-and-withdraw sequence V. Note that ${}^{R}\boldsymbol{\alpha}$ and ${}^{S}\boldsymbol{\alpha}$ have no subscript $(\rightarrow)$ due to associativity (cf. Remark 1).

Furthermore, each vector ${}^{S^k}\boldsymbol{a}$ in (11) is defined as

$$
({}^{S^k}\boldsymbol{a})^T\boldsymbol{z} := -\frac{1}{\dot{\gamma}^-} D_1\gamma^- \cdot \boldsymbol{z} \qquad (19)
$$

with $\dot{\gamma}^-$ and $D_1\gamma^-$ as in (16) and (18), respectively. ▲

Although straightforward to obtain, the general form of ${}^{p\leftarrow a}\boldsymbol{H}$ for a character-n event is not presented here due to space limitations and will be detailed in a future publication.

***Remark** 2:* Whenever the transition $s^+ \leftarrow s^-$ in the sequence S^k corresponds to multiple switching function activations (e.g,. $S^1 = {}^{(21)}S^1 = 11 \leftarrow 00$, with $s^+ = 11$ and $s^- = 00$), it is understood that $\gamma^{\eta(s^+\leftarrow s^-)}$ in (18) should be interpreted as one of the switching functions that become active during the transition (continuing the example, $S^1 = {}^{(21)}S^1$, $\eta(s^+ \leftarrow s^-) = \{10, 01\}$ so that $\gamma^{\eta(s^+\leftarrow s^-)}$ in (18) means γ^{10} or γ^{01}). Straightforwardly to verify, the choice does not affect the final value of ${}^{p\leftarrow a}\boldsymbol{h}$ in (9). △

***Remark** 3:* The gain ${}^{p\leftarrow a}\boldsymbol{H}$ appearing in Definition 4 is *positively homogeneous of order zero* with respect to $\boldsymbol{z}$ (${}^{p\leftarrow a}\boldsymbol{H}(\lambda\boldsymbol{z}, t) = {}^{p\leftarrow a}\boldsymbol{H}(\boldsymbol{z}, t)$, for any $\lambda \ge 0$) because positive scalar multiplications do not affect the inequality conditions used to define it. This makes ${}^{p\leftarrow a}\boldsymbol{h}(\boldsymbol{z}, t)$ a positively homogeneous function (of order one), explaining the name given to the time-triggered approximation of the hybrid dynamics about a nominal trajectory. △

The positive homogenization provides a first-order approximation of the hybrid system's trajectories that are in a neighborhood of the associative transversal nominal trajectory $(\boldsymbol{\alpha}, \boldsymbol{\mu})$. This result is illustrated graphically in Fig. 2 and stated formally as follows.

***Theorem** 1 (First-order accuracy):* Consider an associative transversal nominal trajectory $(\boldsymbol{\alpha}(t,i), \boldsymbol{\mu}(t,i))$ of (1)-(2) with push-and-withdraw sequence V over the time interval $t \in [t_0, t_f]$. Let $\bar{\boldsymbol{\mu}}(t,i)$ be a chosen continuous extension of $\boldsymbol{\mu}(t,i)$ with corresponding state extension $\bar{\boldsymbol{\alpha}}(t,i)$. Denote with $\boldsymbol{x}_\varepsilon(t,i,k)$ the ε-parametrized family of trajectories satisfying (1)-(2) with initial condition $\boldsymbol{x}_\varepsilon(t_0,0,0) = \boldsymbol{\alpha}_0 + \varepsilon\boldsymbol{z}_0$ and input $\boldsymbol{u}_\varepsilon(t,i,k) = {}_{\rightarrow}\bar{\boldsymbol{\mu}}(t,i,k) + \varepsilon\bar{\boldsymbol{v}}(t,i,k)$ where $\boldsymbol{\alpha}_0 = \boldsymbol{\alpha}(t_0,0)$, $\boldsymbol{z}_0$ an arbitrary perturbation of the initial condition, ${}_{\rightarrow}\bar{\boldsymbol{\mu}}(t,i,k)$ the input extension based on $\bar{\boldsymbol{\mu}}(t,i)$ induced by the push-and-withdraw sequence V and $\bar{\boldsymbol{v}}(t,i,k)$ an

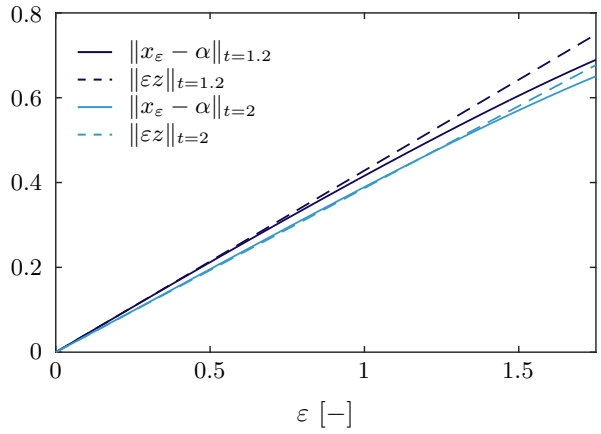

Fig. 3. Norm of the error $(\boldsymbol{x}_\varepsilon - \boldsymbol{\alpha})$ and local approximation $\varepsilon \boldsymbol{z}$ for two time instances (see Fig. 4).

arbitrarily-chosen input perturbation. Theoretically, $\bar{\boldsymbol{v}}(t,i,k)$ should be defined for all $t \in [t_0, t_f]$, $i \in \{0,1,\ldots,N\}$, and $k \in \{0,1,\ldots,c_i\}$, with c_i the character of event i and $N \leq \infty$ the number of nominal macro events of $(\boldsymbol{\alpha}, \boldsymbol{\mu})$. The extension ${}_{\rightarrow}\bar{\boldsymbol{\mu}}(t,i,k)$ equals the pushing input

$$ {}_{\searrow}\bar{\boldsymbol{\mu}}(t,i,k) = \begin{cases} \bar{\boldsymbol{\mu}}(t,i), & k \neq l_{i+1}, \\ \bar{\boldsymbol{\mu}}(t,i+1), & k = l_{i+1}, \end{cases} \tag{20} $$

or the withdrawing input

$$ {}_{\nearrow}\bar{\boldsymbol{\mu}}(t,i,k) = \begin{cases} \bar{\boldsymbol{\mu}}(t,i), & k = 0, \\ \bar{\boldsymbol{\mu}}(t,i+1), & k \neq 0, \end{cases} \tag{21} $$

depending on the value of the i-th entry of the sequence V.

Then, the perturbed trajectory $\boldsymbol{x}_\varepsilon$ can be approximated as

$$ \boldsymbol{x}_\varepsilon(t,i,0) = \bar{\boldsymbol{\alpha}}(t,i) + \varepsilon \bar{\boldsymbol{z}}(t,i) + o(\varepsilon), \quad t^l_{i-1,\varepsilon} \leq t \leq t^1_{i,\varepsilon} \tag{22} $$

where $\bar{\boldsymbol{z}}(t,i)$ denotes the extended solution of (8)-(10) with initial condition $\bar{\boldsymbol{z}}(t_0,0) = \boldsymbol{z}_0$ and input $\bar{\boldsymbol{v}}(t,i) = \bar{\boldsymbol{v}}(t,i,0)$, and where $t^1_{i,\varepsilon}$ denotes the *first* micro event time of $\boldsymbol{x}_\varepsilon$ during the macro event i, and $t^l_{i-1,\varepsilon}$ the *last* micro event time of $\boldsymbol{x}_\varepsilon$ during the macro event $i-1$. □

The proof of Theorem 1 has been removed for space limitations. It can be found in [23, Chapter 5].

IV. The Plank and Box: A Numerical Validation

Consider the animation snapshots depicted on the top row of Fig. 4. They depict a *fully actuated* box of 2 kg and rotational inertia $0.067\ \mathrm{kgm}^2$ with respect to its center of mass forced to impact against a 2.5 m long plank, connected to the fixed world via a revolute joint that includes a torsional spring ($500\ \mathrm{Nm/rad}$) and damper ($500\ \mathrm{Nms/rad}$). The plank inertia about the pivot is $4.5\ \mathrm{kgm}^2$. After an intended flat impact, the block is pushed down along the frictionless surface of the plank and finally comes at rest. Fig. 4 also shows the state norm as a function of time, illustrating the state jump after the impact. Starting from $\boldsymbol{\alpha} \in \mathbb{R}^8$ (it is a 4 DoF mechanism) and corresponding input $\boldsymbol{\mu} \in \mathbb{R}^3$ (full actuation of the box), we employ the tracking control law

$$ \boldsymbol{u} = {}_{\rightarrow}\bar{\boldsymbol{\mu}} + \boldsymbol{K}({}_{\rightarrow}\bar{\boldsymbol{\alpha}} - \boldsymbol{x}) \tag{23} $$

where all quantities, including the matrix gain $\boldsymbol{K}$, are a function of the multiscale hybrid time (t,i,k) and where ${}_{\rightarrow}\bar{\boldsymbol{\alpha}}$ and ${}_{\rightarrow}\bar{\boldsymbol{\mu}}$ are the extended nominal state and input trajectories based on the chosen push-and-withdraw sequence V (cf. Definitions 2 and 3 and statement of Theorem 1). Assuming, as reasonable to expect in actual physical situations, that the state is *not* available during micro transitions and that only the beginning and end of the micro events' time interval can be detected, the feedback gain $\boldsymbol{K}(t,i,k)$ will be set to zero for $k \neq \{0,l\}$, with l denoting the last micro event index. Regarding ${}_{\rightarrow}\boldsymbol{\mu}$ in (23), while making contact, we keep the same (pushing) feedforward input until full contact is established (i.e., $V = \{\searrow\}$)

Using (23), we place the box in a perturbed initial condition $\boldsymbol{x}_0 = \boldsymbol{\alpha}_0 + \boldsymbol{z}_0$ (cf. Fig. 4) and compare the system's response $\boldsymbol{x}$ with its corresponding first-order approximation $\boldsymbol{\alpha} + \boldsymbol{z}$ obtained via the positive homogenization. Fig. 4 clearly indicates that the positive homogenization provides an accurate approximation of the behavior of the system about the nominal trajectory, past the micro event sequence. To further support this conclusion and to illustrate that the positive homogenization indeed provides a first-order approximation, we consider the initial conditions $\boldsymbol{x}_0 + \varepsilon \boldsymbol{z}_0$ for a range of ε and plot both the error norm $\|\boldsymbol{x}_\varepsilon - \boldsymbol{\alpha}\|$ and its approximation $\|\varepsilon \boldsymbol{z}\|$ for two time instances occurring after the impact transition. The results can be seen in Fig. 3 confirming the first-order approximation result of Theorem 1. The reader is referred to [24] for full details about the numerical simulation, including the validation of associativity.

V. Conclusions

This paper has presented a novel sensitivity analysis about a nominal trajectory with simultaneous impacts. Future contributions will highlight the usefulness of such a tool for control design and stability analysis.

References

[1] R. Goebel, R. G. Sanfelice, and A. R. Teel, *Hybrid Dynamical Systems*. Princeton: Princeton University Press, 2012.

[2] J. J. B. Biemond, N. van de Wouw, W. P. M. H. Heemels, and H. Nijmeijer, "Tracking control for hybrid systems with state-triggered jumps," *IEEE Transactions on Automatic Control*, vol. 58, no. 4, pp. 876–890, 2013.

[3] R. Ronsse, P. Lefévre, and R. Sepulchre, "Sensorless stabilization of bounce juggling," *IEEE Transactions on Robotics*, vol. 22, no. 1, pp. 147–159, 2006.

[4] B. Morris and J. W. Grizzle, "Hybrid invariant manifolds in systems with impulsive effects with application to periodic locomotion in bipedal robots," *IEEE Transactions on Automatic Control*, vol. 54, no. 8, pp. 1751–1764, 2009.

[5] A. Johnson, S. Burden, and D. Koditschek, "A hybrid systems model for simple manipulation and self-manipulation systems ," *The International Journal of Robotics Research*, vol. 35, no. 11, pp. 1354–1392, 2016.

[6] J. Reher, E. A. Cousineau, A. Hereid, C. M. Hubicki, and A. D. Ames, "Realizing dynamic and efficient bipedal locomotion on the humanoid robot durus," in *2016 IEEE International Conference on Robotics and Automation (ICRA)*, 2016, pp. 1794–1801.

[7] Y. Gu, B. Yao, and C. S. George Lee, "Exponential stabilization of fully actuated planar bipedal robotic walking with global position tracking capabilities," *ASME Journal of Dynamic Systems, Measurement, and Control*, vol. 140, no. 051008, pp. 1–11, 2018.

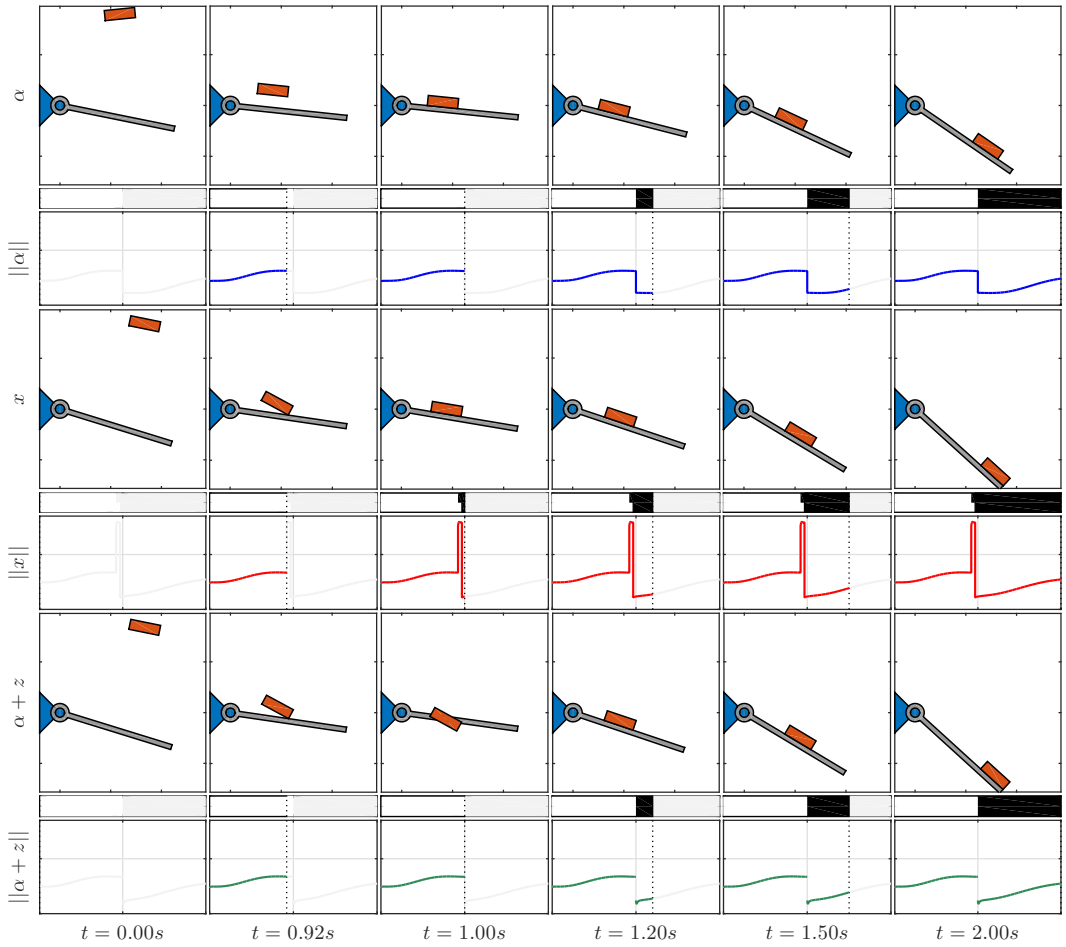

Fig. 4. Illustration of the first-order-approximation theorem via a numerical simulation of the plank and box system. As the second and third rows of animation snapshots show, the perturbed trajectory $\boldsymbol{x}$ with two consecutive impacts (red) is well approximated by the sum of the nominal trajectory $\boldsymbol{\alpha}$ and the positive homogenization $\boldsymbol{z}$ (green), away from the time intervals where micro-events occur. In proximity of micro-events, the approximation $\boldsymbol{\alpha} + \boldsymbol{z}$ can be physically inconsistent (see third snapshot of $\boldsymbol{\alpha} + \boldsymbol{z}$). The horizontal black and white bars illustrate the mode descriptors (black = 1, white = 0).

[8] A. Saccon, N. van de Wouw, and H. Nijmeijer, "Sensitivity analysis of hybrid systems with state jumps with application to trajectory tracking," in *Proceedings of the 53rd IEEE Conference on Decision and Control*, December 2014, pp. 3065–3070.

[9] M. Rijnen, E. de Mooij, S. Traversaro, F. Nori, N. van de Wouw, A. Saccon, and H. Nijmeijer, "Control of humanoid robot motions with impacts: Numerical experiments with reference spreading control," in *IEEE International Conference on Robotics and Automation (ICRA)*, 2017, pp. 4102–4107.

[10] M. W. L. M. Rijnen, J. J. B. Biemond, N. van de Wouw, A. Saccon, and H. Nijmeijer, "Hybrid systems with state-triggered jumps: Sensitivity-based stability analysis with application to trajectory tracking," *IEEE Transactions on Automatic Control*, 2018, under revision, pre-print available at https://hal.archives-ouvertes.fr/hal-01727842v2.

[11] C. G. Cassandras, D. L. Pepyne, and Y. Wardi, "Optimal control of a class of hybrid systems," *IEEE Transactions on Automatic Control*, vol. 46, no. 3, pp. 398–415, 2001.

[12] K. Mombaur, "Using optimization to create self-stable human-like running," *Robotica*, vol. 27, pp. 321–330, 2009.

[13] F. Farshidian, M. Neunert, A. W. Winkler, G. Rey, and J. Buchli, "An efficient optimal planning and control framework for quadrupedal locomotion," in *IEEE International Conference on Robotics and Automation (ICRA)*, 2017, pp. 93–100.

[14] K. A. Khan and P. I. Barton, "Generalized derivatives for hybrid systems," *IEEE Transactions on Automatic Control*, vol. 62, no. 7, pp. 3193–3208, 2017.

[15] A. M. Pace and S. A. Burden, "Decoupled limbs yield differentiable trajectory outcomes through intermittent contact in locomotion and manipulation," in *IEEE International Conference on Robotics and Automation (ICRA)*, 2017, pp. 2261–2266.

[16] ——, "Piecewise-differentiable trajectory outcomes in mechanical systems subject to unilateral constraints," in *International Conference on Hybrid Systems: Computation and Control*, 2017, pp. 243–252.

[17] R. I. Leine and N. van de Wouw, *Stability and Convergence of Mechanical Systems with Unilateral Constraints*. Berlin: Springer Verlag, 2008, vol. 36 of Lecture Notes in Applied and Computational Mechanics.

[18] B. Brogliato, *Nonsmooth Mechanics. Models, Dynamics and Control*, 2nd ed. Berlin: Springer, 1999.

[19] I. C. Morarescu and B. Brogliato, "Trajectory tracking control of multiconstraint complementarity lagrangian systems," *IEEE Transactions on Automatic Control*, vol. 55, no. 6, pp. 1300–1313, 2010.

[20] V. Acary and B. Brogliato, *Numerical Methods for Nonsmooth Dynamical Systems*. Springer, 2008.

[21] M. di Bernardo, C. Budd, A. Champneys, and P. Kowalczyk, *Piecewise-smooth Dynamical Systems: Theory and Applications*. London: Springer Verlag, 2008.

[22] M. W. L. M. Rijnen, A. Saccon, and H. Nijmeijer, "On optimal trajectory tracking for mechanical systems with unilateral constraints," in *Proceedings of the 54th IEEE Conference on Decision and Control*, Osaka, Japan, December 2015, pp. 2561–2566.

[23] M. W. L. M. Rijnen, "Enabling motions with impacts in robotic and mechatronic systems," Ph.D. dissertation, Dept. of Mechanical Engineering, Eindhoven University of Technology (TU/e), online available at research.tue.nl, 2018.

[24] H. L. Chen, "Tracking control for mechanical systems experiencing simultaneous impacts," Master's thesis, Dept. of Mechanical Engineering, Eindhoven University of Technology, Eindhoven, January 2018, https://tinyurl.com/ybv2uxyc.